

Article

Nano-TiO₂ in Hydraulic Lime–Metakaolin Mortars for Restoration Projects: Physicochemical and Mechanical Assessment

Kali Kapetanaki, Chrysi Kapridaki  and Pagona-Noni Maravelaki * 

School of Architecture, Technical University of Crete, Polytechnioupolis, Akrotiri, 73100 Chania, Crete, Greece; kapetanaki.kali@gmail.com (K.K.); ckapridaki@gmail.com (C.K.)

* Correspondence: pmaravelaki@isc.tuc.gr

Received: 21 October 2019; Accepted: 14 November 2019; Published: 19 November 2019



Abstract: In recent years, lime mortars mixed with artificial or natural pozzolans are commonly used in restoration applications. The aim of this work is the assessment of carbonation, pozzolanic reaction, setting time, and mechanical properties of metakaolin–lime mortars mixed with crystalline nano-titania (nT) as additive. The studied mortars consist of hydrated lime and metakaolin in 60/40 ratio (wt%) and fine aggregates of either carbonate or silicate sand. The concentration of the nano-titania is equal to 6 (wt%) of the binder. For comparison purposes, three types of mortars and pastes are designed: Without the addition of nano-titania, with nT activated or not under UV irradiation. The evaluation of the carbonation and pozzolanic reaction over a 1.5-year curing period is carried out through thermal analysis (DTA/TG), infrared spectroscopy (FTIR) and X-ray diffraction analysis (XRD). The uniaxial compression and the three-point bending tests at 28 days, 3 months, and 6 months were carried out to evaluate mechanical properties. The addition of activated nano-titania, due to an increased photocatalytic activity, accelerated the setting of the mortars, improving at the same time the mechanical properties. The plastic behavior of the lime–metakaolin mortars with activated nT was attributed to the evolution of carbonation and pozzolanic reaction.

Keywords: lime–metakaolin mortars; carbonation; pozzolanic reaction; setting time; nano-TiO₂

1. Introduction

In restoration projects of historical buildings, the selection of repair materials, in order to achieve the optimum performance after rehabilitation, is very critical. The raw materials used in such constructions have been mainly stones, bricks, as well as lime and soil mortars [1]. Therefore, lime mortars mixed with pozzolans are compatible materials to historical buildings, owing to their physicochemical, structural, and mechanic characteristics [2]. As opposed to the above, in past decades, the use of cement has prevailed due to high mechanical strength, workability, and accelerated setting time compared with lime mortars [3]. However, the use of such materials has caused damages to monuments, due to incompatibility in porosity, pore size and mechanical properties, high salt content, limited elasticity, etc. [4,5]. In order to enhance the compatibility between the ancient components and the new mortars, various materials such as brick, tiles, pottery, and tuff dust have been studied as additives to the pozzolanic mortars, showing improved mechanical properties [6–8].

Mortars are also widely used as an adhesive material for joining fragments of archaeological interest. Such mortars should have quick setting and hardening time and, most importantly, adhesion capability and lower strength than the substrate, in order to ensure that any failure will take place on the adhesive interface [9,10].

Additionally, a critical agent that causes deterioration to cultural heritage constructions is the increasing air pollution. Atmospheric pollutants are deposited on architectural surfaces, causing

decay via erosion, recession, and crust formation. For the purpose of the optimum maintenance of building substrates, advanced consolidants and protective agents based on nanotechnology have been developed [11]. Among these materials, the self-cleaning products possess a predominant role as a protective treatment for stones and mortars [11]. Into this direction, coatings and mortars with self-cleaning properties have been specifically designed, tailoring to prevent and/or to decompose black crusts [12,13]. Nano-TiO₂ has been incorporated as additive in mortars, due to its photocatalytic property, resulting in self-cleaning and quick-hardening plasters with high mechanical properties [14]. The addition of either pure nano-TiO₂ or doped TiO₂ with Fe/V into lime mortars and coatings has been proved that it plays a significant role as an effective agent for the decomposition of air pollutants under UV and Vis irradiation [15,16].

In this work, nano-titania (nT) composed of anatase (90%) and rutile (10%) forms was added in the designed mortars consisting of hydrated lime (L), metakaolin (M), and fine aggregates of carbonate (N) or silicate (P) nature. The already established photocatalytic activity of nT enhanced the hydration and carbonation process, thus improving the mortars mechanical properties and providing self-cleaning characteristics [17,18]. The nT was activated under UV irradiation for 15 min. The purpose of this research was to investigate the effect of nT in the hydration and carbonation and, therefore, in the mechanical properties of the mortars. Furthermore, the addition of nano-titania provided mortars with accelerated setting time, as carbonation took place in earlier stages, but without hindering pozzolanic reaction. The assessment of carbonation and pozzolanic reaction during a year of curing time was carried out through thermal analysis (DTA/TG), infrared spectroscopy (FTIR), and X-ray diffraction (XRD) analysis.

2. Materials and Methods

2.1. Mortar Mixes Design

In the adhesive mortar design, hydrated lime (L; by CaO Hellas) mixed with metakaolin (M; Metastar 501 by Imerys) and nano-titanium dioxide (nT; nano-structured nano-titania by NanoPhos) as a photocatalytic additive were proposed.

Table 1 shows the mortar mixes, weight ratios, percentage of L, M, and nT in wt%, the water/binder ratio, as well as the flow table consistency determined according to EN 1015-3. A ratio of water to binder (W/B) was approximately equal to 6:5. The mixing tools and materials were stored at a constant temperature of 23 °C for 24 hours before mixing. To ensure the ongoing pozzolanic reaction, the quantity of L that will react with M was in a weight ratio equal to 6:4. In order to overcome the increased water demand of nano-additives and to avoid agglomerates formation, the nT was dispersed into water under intensive stirring for 15 min. The obtained TiO₂ colloidal solution was subjected to UV radiation (365 nm) for 20 min to activate the nT. Then, it was added to the other raw materials and stirred with a handheld mixer for 5 min. The MLT samples subjected to UV treatment are presented with the “uv” prefix. For comparison purposes, another set of MLT mortars with nT, not subjected to the UV treatment, was designed. The selected aggregates were of carbonate and siliceous nature with a grain size ranging from 2 to 0.06 mm, according to standard sands specifications. The flow design for all mixes ranged from 136 to 148 mm. It was expected that the fluidity of ML mortars was decreased by nT.

Table 1. Mortar mixes (composition in wt%).

	Code	Binder		TiO ₂	Aggregates				Consistency (mm)
		L	M		Carbonaceous	Silicate	B/A	W/B	
MORTARS	MLN	60	40	-	100	-	1	1.25	136.96
	MLNT	60	40	6	100	-	1	1.19	136.52
	MLNTuv	60	40	6	100	-	1	1.19	135.94
	MLP	60	40	-	-	100	1	1.35	148.12
	MLPT	60	40	6	-	100	1	1.20	138.25
	MLPTuv	60	40	6	-	100	1	1.22	137.16
PASTES	ML	60	40	-	-	-	-	1.75	-
	MLT	60	40	6	-	-	-	1.65	-
	MLTuv	60	40	6	-	-	-	1.65	-

2.2. Evaluation of Mixtures

The mixtures were molded in prismatic and cubic molds (4 × 4 × 16 cm and 5 × 5 × 5 cm) according to EN 196 standard, for mechanical tests, uniaxial compression, and the three-point bending tests. After molding, the specimens were stored in a curing chamber with a temperature of 23 ± 2 °C and relative humidity of 50 ± 5%.

Compressive strength (Fc) and flexural strength were measured by uniaxial compression and the three-point bending strength (Ff-3pb), respectively, according to EN 1015-11:1999. The modulus of elasticity and toughness was determined by the strain–stress curve of compression testing.

For the physico-chemical assessment, pastes of 5 mm in diameter × 30 mm in height were prepared and sealed into ceramic tubes; the latter were subsequently submerged in acetone to stop the setting process at different periods.

In powder paste samples, the evolution of hydration and carbonation was examined with XRD, FTIR, and DTA/TG. The mineralogical analysis was carried out by X-ray powder diffraction analysis (XRD) on a Bruker D8 Advance Diffractometer, using Ni-filtered Cu Kα radiation (35 kV 35 mA) and a Bruker Lynx Eye strip silicon detector. DTA/TG was operated with a Setaram LabSys Evo 1600 °C thermal analyzer, in static air atmosphere up to 1000 °C at a rate of 10 °C/min. FTIR analysis was performed in an FTIR Perkin-Elmer 1000 spectrometer with a resolution of 4 cm⁻¹ in the spectral range of 400–4000 cm⁻¹. The reflectance spectra of the synthesized pastes were obtained using a UV-Vis Perkin-Elmer Lambda 35 spectrophotometer (Perkin-Elmer, Waltham, MA, USA) in wavenumber range of 900–190 nm.

The Vicat apparatus was used for measuring the initial and final time of setting of mortar mixes, according to the method proposed in ASTM C807.

3. Results and Discussion

3.1. Physico-Chemical Study

3.1.1. Thermal Analysis (DTA)

In order to evaluate carbonation and pozzolanic reaction through thermal analysis, calcium hydroxide Ca(OH)₂ (CH) was determined according to a methodology proposed by Gameiro et al. [19], using the following equations:

$$CH_{poz} = CH_{th} - (CH_{fr} + CH_{carb}) \quad (1)$$

$$CH_{fr} = CH_{ach} \times \frac{Mm(CH)}{Mm(H_2O)} \quad (2)$$

$$CH_{carb} = Ca_{dec} \times \frac{Mm(CH)}{Mm(CO_2)} \quad (3)$$

where CH_{poz} and CH_{carb} are considered as the consumption of CH due to pozzolanic reaction and carbonation, respectively; CH_{th} is the initial mass of lime into the paste; CH_{fr} is the free portlandite; CH_{deh} is the mass loss referred to as the dehydration of CH at 360–560 °C, shown in Figure 1a; Ca_{dec} is the mass loss referred to as the decomposition of calcium carbonate at 600–900 °C, as illustrated Figure 1b; and, finally, M_m is the molar mass. The carbonation evolution illustrated in Figure 1a reveals that on the 15th day, nTuv pastes exhibited higher CH consumption compared to ML and MLT pastes. On the other hand, Figure 1b reveals that the CH consumed in pozzolanic reaction on the 15th day had the smallest value for the MLTuv paste, contrary to what was observed for the other two pastes. After 21 days, a similar trend is observed for all of the pastes, both in carbonation and pozzolanic reaction.

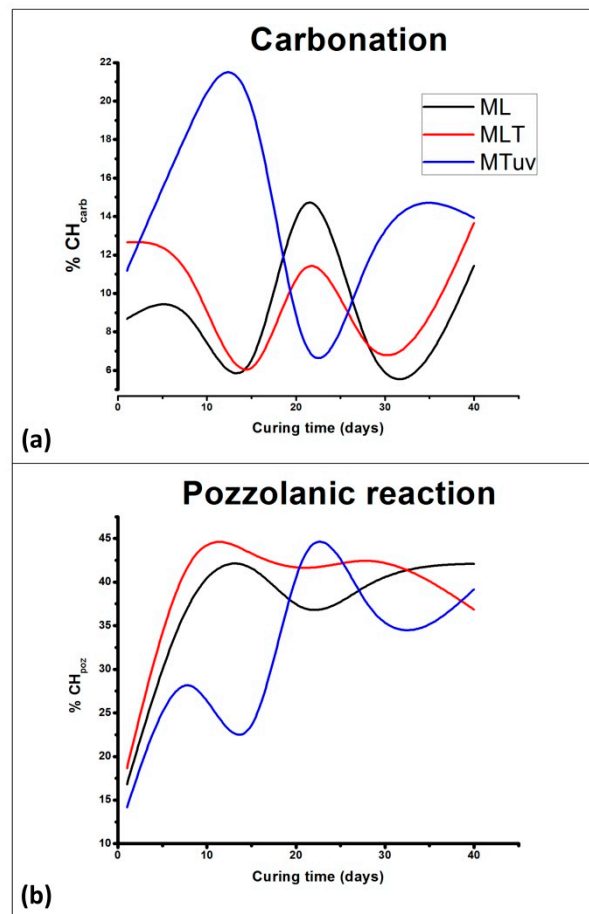


Figure 1. %CH consumption during the (a) carbonation and (b) pozzolanic reactions after 1, 15, 21, 28, and 40 days of paste aging.

3.1.2. Infrared Spectroscopy (FTIR)

The IR spectra have been used as complementary tools in studying the evolution of carbonation and pozzolanicity. More specifically, in the FTIR spectra, the carbonation and pozzolanic reactions were assessed through the decreasing intensity of the peak, attributed to portlandite (3643 cm^{-1}), and the increasing intensity of calcite (at $1420, 870, 712\text{ cm}^{-1}$), as well as the Si–O–Si formation of hydraulic components ($1050, 990\text{ cm}^{-1}$). The FTIR spectra of MLTuv pastes showed that calcite was produced even on the first day of hydration. Furthermore, as illustrated in Figure 2a, peaks characteristic of the neo-formed hydraulic components, such as 960 cm^{-1} , were predominant on the 15th day of curing, while portlandite was consumed. Especially, it was observed that intensity and sharpness of the bands in the spectral ranges from $1100\text{--}950\text{ cm}^{-1}$ and $550\text{--}400\text{ cm}^{-1}$, both attributed to hydraulic components, were significantly changed. On the first day, the band observed at 1070 cm^{-1} was attributed to amorphous silica of metakaolin; after 15 and 21 days, this band was shifted to $1100\text{--}913\text{ cm}^{-1}$ as a result

of the Si–O asymmetric stretching vibration due to the evolution of the pozzolanic reaction. Moreover, in these time intervals, we noticed a formation of a peak at 423 cm^{-1} that is characteristic for the Al–O vibrations in octahedral sites related to calcium aluminates and aluminosilicate hydrates, as shown in Figure 2b,c [20]. All the aforementioned observations in FTIR spectra indicate that carbonation in MLTuv pastes did not obstacle the pozzolanic reaction.

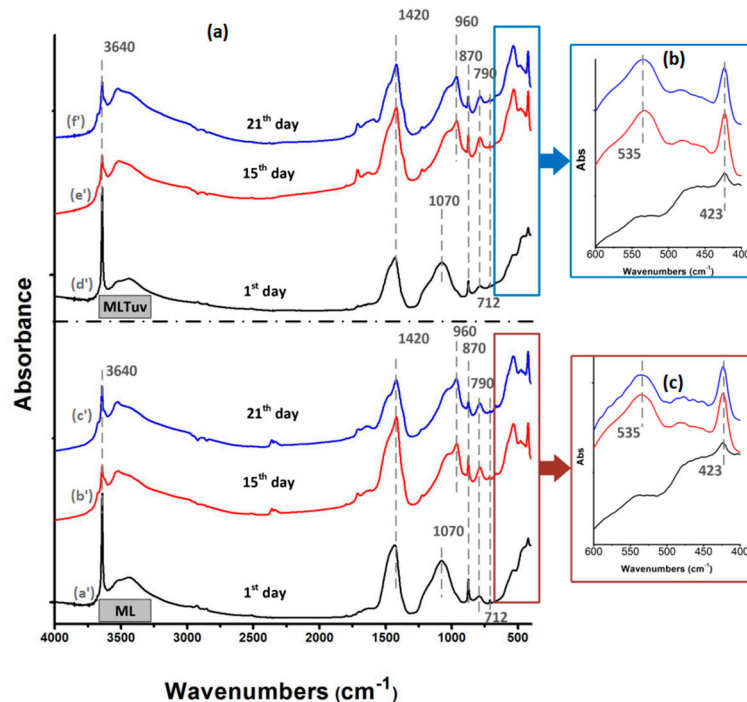


Figure 2. (a) FTIR spectra of ML pastes after (a') 1 day, (b') 15 days, and (c') 21 days of curing time and MLTuv pastes at (d') 1 day, (e') 15 days, and (f') 21 days of curing time. (b) Area of $600\text{--}400\text{ cm}^{-1}$ of MLTuv pastes. (c) Area of $600\text{--}400\text{ cm}^{-1}$ of MLT pastes.

3.1.3. Mineralogical Analysis (XRD)

In mineralogical analysis, carbonation and pozzolanic reaction took place during the first 15 days. In ML mortars, as hydration proceeded through the reaction between L and M, apart from calcite and portlandite, calcium and aluminum–silicate hydrated phases were also identified [21]. Particularly, as shown in Figure 3, on the first day, absorptions related to portlandite were predominant, while after 15 days of curing, calcite and hydraulic compounds (quartz, tobermorite, and calcium aluminum phases) were formed. Moreover, amorphous compounds were more prominent on the first day, in accordance with the results of the FTIR analysis. Finally, calcium aluminum hydrate phases were observed after 15 days of curing. These compounds are expected to create a denser microstructure with lower pore size and high apparent density, thus resulting in increased mechanical properties [22].

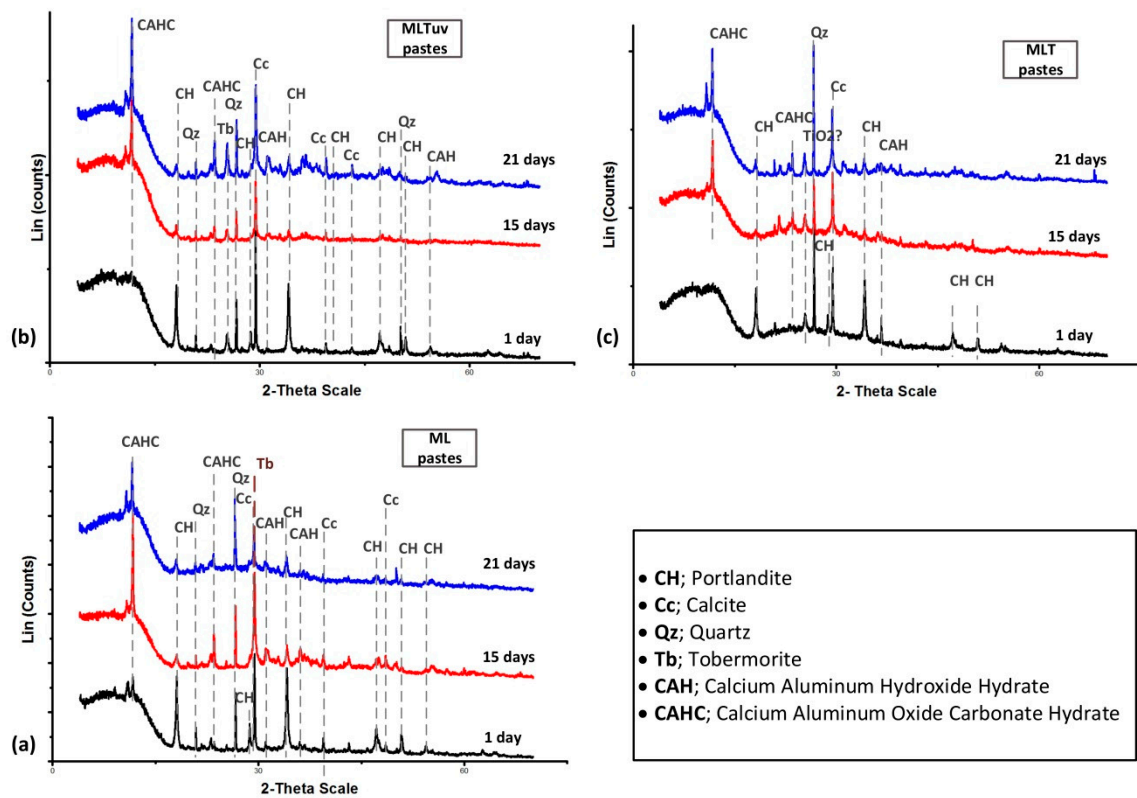


Figure 3. XRD patterns of (a) ML pastes on the 1st day, 15th day, and 21st day. (b) MLT pastes on the 1st day, 15th day, and 21st day. (c) MLTuv pastes on the 1st day, 15th day, and 21st day.

3.1.4. UV-Vis Measurements

Figure 4 reveals that the MLTuv pastes with activated nT showed increased absorption at the UV range, comparing to pure ML pastes and MLT pastes with non-activated nT. These analytical results clearly prove that the initial activation of nT under UV irradiation is a key point in achieving an increased photocatalytic activity in lime pastes. Given that the pastes were unexposed to solar irradiation for one year, it is reasonable to assume that photocatalysis in the MLTuv pastes is maintained at the maximum level.

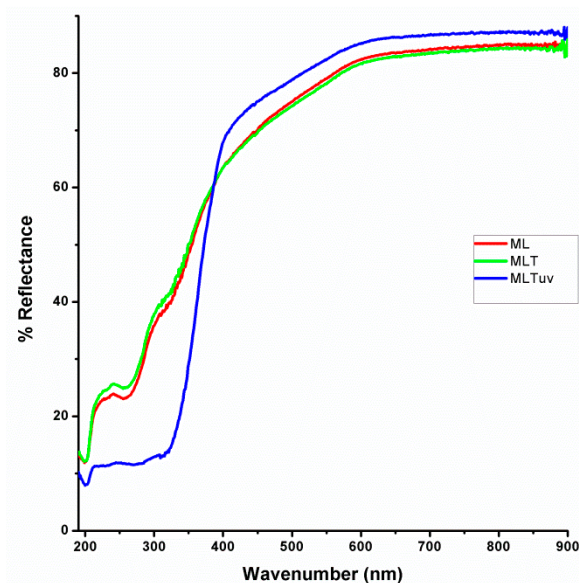


Figure 4. Reflectance of ML, MLT, and MLTuv pastes from 190–900 nm.

3.1.5. Setting Time

In the Vicat test illustrated in Figure 5, the MLTuv samples are well diversified from the other mortars, as they present both the lowest initial and final setting time. This finding further supports the enhancement of carbonation in MLTuv pastes, and therefore, its effect on the hardening of mortar.

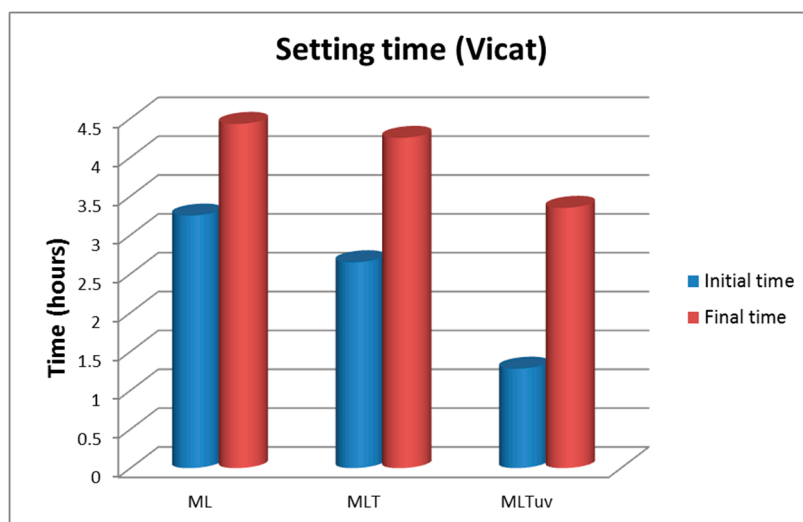


Figure 5. Initial and final time of setting time of pastes ML, MLT, and MLTuv.

3.2. Mechanical Study

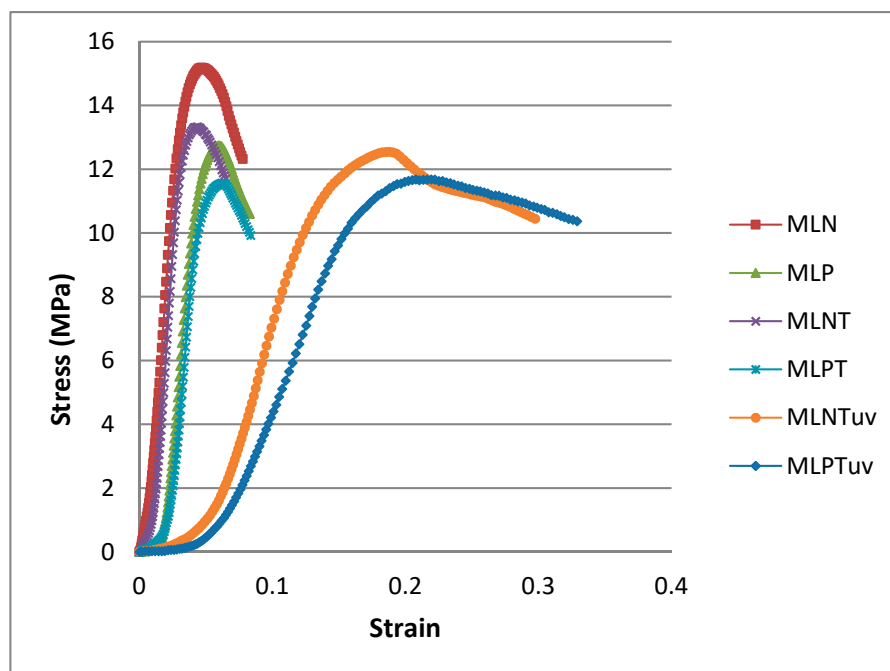
Table 2 presents the mechanical properties of mortars measured at 28 days, 3 months, and 6 months. Mortars exhibited decreased strengths at 3 months, comparing to the corresponding values of 28 days, and increased strength after 6 months. The decrease of F_c values over time in the ML compositions has been already reported by other authors, and was most probably attributed to the microcracking formation due to shrinkage during the curing [23]. However, the decrease in MLT formulations in early curing time may be attributed to the reduction of cohesion between binder and aggregates, due to the presence of an inert additive, such as nano- TiO_2 . This cohesion seems to be reinstated in MLTuv after 90 days of curing, as we noticed that compression strength in the sixth month, exceeding the 28-day resistance and even surpassing the corresponding strength of nT-free and non-activated nT mortars. This conclusion is very critical, as it proves that the addition of nano-titania did not have any harmful impact on the mechanical properties of the mortars. Finally, the mortars with non-activated nT exhibited a similar trend and values to those without nT, indicating that addition of nT without initial activation cannot be considered as beneficial in the whole curing process. Toughness, also defined as energy absorption capacity, was predominant in the nT-modified mortars. Higher values of the modulus of elasticity (E) were recorded for the ML mortars than the nT-modified mortars. The aggregates of carbonate nature provided better mechanical performance than the siliceous aggregates in 28 days of curing.

Table 2. Mechanical properties of the designed mortars.

Code	Curing Time	F _c (MPa) ^a	F _b (MPa) ^b	E (GPa) ^c	Max Strain ^d %	T (J m ⁻³) ^e
MLN	28 days	15.03 (±0.36)	2.96 (±0.28)	0.67	7.93	0.8
	3 months	9.85 (±0.13)	2.63 (±0.5)			
	6 months	12.53 (±2.2)	3.85 (±0.41)			
MLNT	28 days	13.54 (±0.45)	3.82 (±0.28)	0.66	7.12	0.59
	3 months	8.68 (±0.4)	2.48 (±0.33)			
	6 months	11.67 (±0.05)	3.34 (±0.1)			
MLNTuv	28 days	12.57 (±0.2)	3.29 (±0.36)	0.16	29.58	2.39
	3 months	11.35 (±0.03)	1.8 (±0.12)			
	6 months	17.18 (±0.57)	2.53 (±0.35)			
MLP	28 days	12.82 (±0.23)	2.44 (±0.13)	0.53	7.9	0.66
	3 months	10.26 (±2.43)	2.85 (±0.27)			
	6 months	15.29 (±0.22)	3.34 (±0.17)			
MLPT	28 days	11.56 (±0.32)	2.55 (±0.24)	0.43	9.64	0.66
	3 months	10.12 (±0.33)	1.14 (±0.26)			
	6 months	11.06 (±0.36)	3.19 (±0.08)			
MLPTuv	28 days	11.78 (±0.53)	2.70 (±0.19)	0.15	30.48	2.19
	3 months	11.06 (±0.36)	1.30 (±0.57)			
	6 months	15.60 (±0.12)	2.31 (±0.21)			

Mean values of three samples: ^a Compressive strength; ^b three-point bending strength; ^c modulus of elasticity; ^d max strain during compression test; ^e toughness.

The stress–strain curves of uniaxial compression illustrated in Figure 6 reveal that the nTuv mortars exhibited a predominantly plastic behavior, whereas the other mortars behaved in a more brittle manner, a fact that also explains the increased values of modulus of elasticity of ML mortars in comparison with those of nT mortars, as well as lower maximum strain. More specifically, the mortar with carbonate aggregates (MLN) displayed the greatest elastic region, whereas the MLNTuv and MLPTuv mortars showed the smallest elastic regions and the greatest plasticity. It seems that the photo-activated nT, due to its hydrophilicity, created an environment in which carbonation was promoted, whereas the pozzolanic reaction followed.

**Figure 6.** Strain–stress curves of lime–metakaolin mortars at the compression test of 28 days.

4. Conclusions

The activation of nT, used as additive in the lime–metakaolin mortars, promoted the evolution of the carbonation process versus the pozzolanic reaction in the first days of hydration, without obstructing the pozzolanic reaction in the next stages. The fact that carbonation preceded the pozzolanic reaction in nTuv pastes resulted in quick setting times, comparing to both formulations with non-activated nT. Additionally, nTuv mortars exhibited reduced compressive strength up to 3 months of curing, whereas at 6 months, strength was increased. The long-term improvement of nTuv mortars can be attributed to the evolution of the pozzolanic reaction and the reduction in shrinkage by the continued carbonation of part of the hydrated compounds, such as calcium aluminate carbonate, which were prevalent in the nTuv samples, according to the XRD analysis [24]. The carbonation that preceded the pozzolanic reaction seemed to have an effect on the observed plastic behavior and particularly high toughness of the nTuv mortars. The mortars and pastes with non-activated nT exhibited a similar trend to those without nT, indicating the important role played by the activation of nano-TiO₂. Concluding, the addition of nano-TiO₂ in lime–metakaolin formulations resulted in plastic mortars with accelerated setting time and high mechanical strength, appropriate for adhesion of porous stone fragments and filling of holes.

Author Contributions: Conceptualization, P.-N.M.; methodology, P.-N.M., K.K., and C.K.; investigation, K.K. and C.K.; data curation P.-N.M. and K.K.; writing—original draft preparation, P.-N.M. and K.K.; writing—review and editing, P.-N.M.; visualization, P.M. and C.K.; supervision, P.-N.M.; project administration, P.-N.M.; funding acquisition, P.-N.M.

Acknowledgments: The authors would like to thank Stelios Mavrigiannakis, Technical Staff of Lab of Rock Engineering, for his excellent scientific and technical support for mechanical tests. The authors also acknowledge Prof Nikolaos Pasadakis, Eleni Chamilaki, and Antonis Stratakis from TUC for their contribution in chemical and mineralogical analysis, respectively. Finally, the authors also express sincere gratitude to Eleftheria Vazgiouraki for carrying out UV-Vis measurements.

Conflicts of Interest: The authors declare no conflicts of interest.

References

1. Maravelaki-Kalaitzaki, P.; Bakolas, A.; Moropoulou, A. Physico-chemical study of cretan ancient mortars. *Cem. Concr. Res.* **2003**, *33*, 651–661. [[CrossRef](#)]
2. Moropoulou, A.; Bakolas, A.; Anagnostopoulou, S. Composite materials in ancient structures. *Cem. Concr. Compos.* **2005**, *27*, 295–300. [[CrossRef](#)]
3. Ergenc, D.; Fort, R.; Silva, A.S.; Veiga, R.; Arauz, D.S. The effects of DiloCarB as carbonation accelerator on the properties of lime mortars. *Mater. Struct.* **2018**, *51*. [[CrossRef](#)]
4. Apostolopoulou, M.; Aggelakopoulou, E.; Bakolas, A.; Moropoulou, A. Compatible mortars for the sustainable conservation of stone in masonries. In *Advanced Materials for the Conservation of Stone*; Springer: Cham, Switzerland, 2018; pp. 97–123.
5. Papayianni, I.; Stefanidou, M. Durability aspects of ancient mortars of the archeological site of olynthos. *J. Cult. Herit.* **2007**, *8*, 193–196. [[CrossRef](#)]
6. Nežerka, V.; Antoš, J.; Tesárek, P.; Zeman, J. Performance of repair mortars used in bed joints of masonry piers. In *Proceedings of the Civil-Comp Proceedings—15th International Conference on Civil, Structural and Environmental Engineering Computing*, Prague, Czech Republic, 1–4 September 2015.
7. Lippiello, M.; Ceraldi, C.; D’Ambra, C.; Lignola, G.P. Mechanical characterization of ancient pozzolanic mortars with additions of brick and tuff dust: A comparative investigation. In *Proceedings of the 10th International Conference on Structural Analysis of Historical Constructions (SAHC 2016)*, Leuven, Belgium, 13–15 September 2016; pp. 558–564.
8. Aalil, I.; Badreddine, D.; Beck, K.; Brunetaud, X.; Cherkaoui, K.; Chaaba, A.; Al-Mukhtar, M. Valorization of crushed bricks in lime-based mortars. *Constr. Build. Mater.* **2019**, *226*, 555–563. [[CrossRef](#)]
9. Karatasios, I.; Amenta, M.; Kilikoglou, V. Hydraulic mortars for joining archaeological stone fragments—A methodological approach. *Struct. Integr. Procedia* **2018**, *10*, 211–218. [[CrossRef](#)]

10. Szemerey-Kiss, B.; Torok, A. Failure mechanisms of repair mortar stone interface assessed by pull-off strength tests, failure mechanisms of repair mortar stone interface assessed by pull-off strength tests. *Bull. Eng. Geol. Environ.* **2017**, *76*, 159–167. [[CrossRef](#)]
11. Sierra-Fernandez, A.; Gomez-Villalba, L.S.; Rabanal, M.E.; Fort, R. New nanomaterials for applications in conservation and restoration of stony materials: A review. *Mater. Construcción* **2017**, *67*, 107. [[CrossRef](#)]
12. Kapridaki, C.; Verganelaki, A.; Dimitriadou, P.; Maravelaki-Kalaitzaki, P. Conservation of monuments by a three-layered compatible treatment of TEOS-Nano-Calcium oxalate consolidant and TEOS-PDMS-TiO₂ Hydrophobic/Photoactive hybrid nanomaterials. *Materials* **2018**, *11*, 684. [[CrossRef](#)] [[PubMed](#)]
13. Aranzabe, E.; Blanco, M.; Goitandia, A.M.; Vidal, K.; Casado, M.; Cubillo, J. Preparation and characterisation of photocatalytic pigments for architectural mortar based on ultramarine blue. *J. Sol-Gel Sci. Technol.* **2019**, 1–8. [[CrossRef](#)]
14. Senff, L.; Ascensão, G.; Ferreira, V.M.; Seabra, M.P.; Labrincha, J.A. Development of multifunctional plaster using nano-TiO₂ and distinct particle size cellulose fibers. *Energy Build.* **2018**, *158*, 721–735. [[CrossRef](#)]
15. Perez-Nicolas, M.; Navarro-Blasco, I.Í.; Duran, A.; Sirera, R.; Fernandez-Alvarez, J.M.; Alvarez, J.I. Obtaining of self-cleaning repair air lime mortars with photocatalysts. In Proceedings of the En: HMC 2016 4th Historic Mortar Conference Scientific Program, Session XV, Santorini, Greece, 10–12 October 2016.
16. Kapridaki, C.; Xynidis, N.; Vazgiouraki, E.; Kallithrakas-Kontos, N.; Maravelaki-Kalaitzaki, P. Characterization of photoactive Fe-TiO₂ lime coatings for building protection: The role of iron content. *Materials* **2019**, *12*, 1847. [[CrossRef](#)] [[PubMed](#)]
17. Maravelaki, N.; Kapridaki, C.; Lionakis, E.; Verganelaki, A. Improvement of properties of hydraulic mortars with addition of nano-titania. In *Adhesives: Mechanical Properties, Technologies and Economic Importance*; Nova Science: Hauppauge, NY, USA, 2014; Chapter 4; pp. 79–93.
18. Chen, J.; Kou, S.; Poon, C. Hydration and properties of nano-TiO₂ blended cement composites. *Cem. Concr. Compos.* **2012**, *34*, 642–649. [[CrossRef](#)]
19. Gameiro, A.; Santos Silva, A.; Grilo, J.; Branco, T.; Veiga, R.; Velosa, A. Physical and chemical assessment of lime–metakaolin mortars: Influence of binder: Aggregate ratio. *Cem. Concr. Compos.* **2014**, *45*, 264–271. [[CrossRef](#)]
20. Duran, A.; González-Sánchez, J.F.; Fernández, J.M.; Sirera, R.; Navarro-Blasco, I.; Alvarez, J.I. Influence of two polymer-based Superplasticizers (poly-naphthalene sulfonate, PNS, and lignosulfonate, LS) on compressive and flexural strength, freeze-thaw, and sulphate attack resistance of lime-metakaolin grouts. *Polymers* **2018**, *10*, 824. [[CrossRef](#)] [[PubMed](#)]
21. Yu, P.; Kirkpatrick, R.J.; Poe, B.; McMillan, P.F.; Cong, X. Structure of calcium silicate hydrate (C-S-H): Near-, mid-, and far-infrared spectroscopy. *J. Am. Ceram. Soc.* **1999**, *82*, 742–748. [[CrossRef](#)]
22. Kaklis, K.; Maurigiannakis, S.; Agioutantis, Z.; Maravelaki-Kalaitzaki, P. Characterization of pozzolanic lime mortars used as filling material in shaped grooves for restoring member connections in ancient monuments. *Int. J. Archit. Herit.* **2018**, *12*, 75–90. [[CrossRef](#)]
23. Maravelaki-Kalaitzaki, P.; Agioutantis, Z.; Lionakis, E.; Stavroulaki, M.; Perdikatsis, V. Physico-chemical and mechanical characterization of hydraulic mortars containing nano-titania for restoration applications. *Cem. Concr. Compos.* **2013**, *36*, 33–41. [[CrossRef](#)]
24. Amenta, M.; Karatasios, I.; Maravelaki, P.; Kilikoglou, P. Monitoring of self-healing phenomena towards enhanced sustainability of historic mortars. *Appl. Phys.* **2016**, *122*, 554. [[CrossRef](#)]

